Research Square

Preprints are preliminary reports that have not undergone peer review.
They should not be considered conclusive, used to inform clinical practice,
or referenced by the media as validated information.

Persistence of the coral *Porites harrisoni* in the Persian/Arabian Gulf is underpinned by strong selection on few genomic loci

Anna Fiesinger

fiesingeranna@gmail.com

University of Konstanz

Rachel Alderdice

University of Konstanz https://orcid.org/0000-0002-4234-7673

Luigi Colin

University of Konstanz https://orcid.org/0000-0002-6966-2817

Gabriela Perna

https://orcid.org/0000-0003-1197-9560

Hannah Manns

University of Konstanz

Samantha Goyen

Australian Institute of Marine Science

Line Bay

Australian Institute of Marine Science https://orcid.org/0000-0002-9760-2977

Nitin Baliga

Institute for Systems Biology https://orcid.org/0000-0001-9157-5974

Jacob Valenzuela

ISB

Daniel Barshis

NOAA

Iliana Baums

Helmholtz Institute of Functional Marine Biodiversity (HIFMB) at the University of Oldenburg
https://orcid.org/0000-0001-6463-7308

John Burt

New York University Abu Dhabi https://orcid.org/0000-0001-6087-6424

Christian Voolstra

University of Konstanz

Article

Keywords: thermal tolerance, climate change, extreme environments, population genetics

Posted Date: July 13th, 2026

DOI: https://doi.org/10.21203/rs.3.rs-10100933/v1

License: This work is licensed under a Creative Commons Attribution 4.0 International License.
Read Full License

Additional Declarations: There is **NO** Competing Interest.

Abstract

Coral reefs are facing catastrophic losses under accelerating ocean warming, with many species already living close to their upper thermal limits. To investigate the genomic basis of thermal tolerance in reef-building corals from extreme environments, this study examined population structure, specificity of host-algal associations, and candidate genomic regions under positive selection in the stony coral *Porites harrisoni* from two sites in the environmentally extreme Persian/Arabian Gulf (PAG) and one site in the neighboring, environmentally more benign, Gulf of Oman (GO). We sampled a total of 119 colonies (*n* = 79 from the two PAG sites, *n* = 40 from the GO site) and subjected them to whole genome shotgun sequencing. Population genetic analyses revealed overall low genetic differentiation between the three sampling locations, with admixture analysis suggesting that the PAG populations trace back to an ancestral lineage distinct from that of the GO. Host genetic variation correlated significantly with algal symbiont assemblage for colonies from the PAG associated with *Cladocopium thermophilum*, highlighting that both host genetics and environment contribute to symbiont specificity. We identified two genomic regions under positive selection in *P. harrisoni* from the PAG, containing 23 annotated genes with highly differentiated SNPs driven to near-fixation, arguing for their essential role in the persistence of genotypes carrying these alleles in an environment this extreme. Our findings suggest that strong directional selection acting on a small set of alleles has disproportionately shaped the genomic architecture of *P. harrisoni* in the PAG, highlighting the importance of conserving regional coral genetic diversity. This study provides a first step in identifying genomic targets for future active intervention strategies (e.g., assisted gene flow through selective breeding) aimed at enhancing coral resilience, while emphasizing the reduced genetic diversity associated with coral adaptation under environmental extremes.

Introduction

Projections for coral reef ecosystems under accelerating climate change are dire, with catastrophic losses anticipated even under more benign scenarios [1]. Current estimates suggest that up to 99% of reef-building coral species could disappear by the end of the century [2]. Reef-building corals already live close to their upper thermal limits, leaving them with little margin to accommodate any further warming [3–5]. Consequently, marine heatwaves frequently trigger bleaching events and mortality [6], driving population declines and threatening over a third of reef-building coral species with local or global extinction [7,8].

To more accurately project future scenarios and inform possible mitigation strategies, corals in thermally extreme environments such as the Persian/Arabian Gulf (PAG) provide invaluable study systems. The PAG is one of the hottest marine environments inhabited by reef-building corals. Due to its restricted inflow of milder surface waters from the Strait of Hormuz [9], this shallow and semi-enclosed ocean basin has already reached seawater temperatures projected for reefs elsewhere at the end of the century [10,11]. For instance, summer maxima exceed 34°C for several consecutive weeks annually [10,12], surpassing the

thermal limits of nearly all other coral reef ecosystems of the tropics by more than 2°C [11,13]. Such prolonged and elevated temperatures, coupled with high salinities [9,14], especially in the southern basin of the PAG, represent a unique selective landscape, imposing strong selective pressures on coral populations within the PAG. Moreover, the PAG is a relatively young sea (approx. 6ka) [15], implying that corals and their algal symbionts had little time to adapt to such extremes [16,17]. This in turn suggests that selection has acted strongly on standing genetic variation to favor heat-tolerant genotypes already adapted to the local prevailing conditions [17,18].

Porites harrisoni is among the few corals that survive these harsh conditions [8] and it is endemic to the Arabian Seas [19]. The exceptional thermal tolerance of PAG corals compared to conspecifics elsewhere has been linked to several factors, such as their association with the heat tolerant symbiont *Cladocopium thermophilum* [5,20,21], osmolytes as a protective mechanisms against high salinity levels [16,22], epigenetic processes [18], and unique adaptive genomic signatures [18,23,24]. For instance, signatures of positive selection in *Platygyra daedalea* could be associated with genes linked to differential expression between bleaching-sensitive and bleaching-resistant colonies, heat tolerance, and larval survival at elevated temperatures [18].

The heritability of such traits associated with thermal tolerance provides a pathway for active intervention [25], as coral populations from extreme thermal environments such as the PAG could provide valuable alleles for assisted gene flow [24,26,27]. Indeed, studies have shown that gametes from heat-adapted corals carry alleles conferring elevated thermal tolerance [28,29], which can be introduced into cooler populations by means of selective breeding where such alleles are rare [24]. However, *P. harrisoni* already lives perilously close to its upper thermal tolerance threshold [5], underscoring the urgency of preserving alleles associated with their exceptional thermal tolerance. This underscores the importance of conserving regional coral genetic diversity to maintain future adaptive potential and implement active interventions [18,25,30].

To date, little is known about the population genetic structure and genomic signatures of selection in *P. harrisoni* in the PAG, one of the few remaining abundant and widespread coral species in this region [31]. Understanding allelic distinctiveness and genetic connectivity between the reefs of the PAG with the neighboring Gulf of Oman (GO) and the Indian Ocean at large is therefore of importance. Here, we conducted population genomic analyses of two reef sites of *P. harrisoni* in the environmentally extreme PAG and one site in the neighboring, more environmentally benign GO, assessed the specificity of host-symbiont assemblages, and identified candidate genes of positive selection to further understand the genomic basis of thermal tolerance and inform active interventions in corals from the PAG.

Material & methods

Sample collection, DNA extraction, and DNA sequencing

Samples of the coral species *Porites harrisoni* (*n* = 119) were collected from two locations in the Persian/Arabian Gulf (Al Saada Reef, SA: 24.085250, 52.243333; Saadiyat Reef, SY: 24.599528, 54.422667) and one location in the Gulf of Oman (Al Aqah, AA: 25.491694, 56.363861) in May/June 2022. Al Aqah is also known as Snoopy Island, so AA and SI are interchangeably used in supplementary datasets and sample names. At each location, samples were collected using SCUBA at depths of 2–11 m (*n* = 39 to 40 colonies per location). Coral colonies were sampled approximately 5 m apart from each other to minimize sampling clonal genotypes [32]. Coral plugs (~ 2 cm diameter) from each colony were drilled with a Nemo V2 Divers Edition underwater drill (Nemo Power Tools LLC, Nevada, USA) fitted with a 2 cm diameter diamond tip core drill bit. Samples were stored in sealable plastic bags upon underwater collection and transported to shore in a cooler filled with seawater from the respective site. Coral fragments were incubated in DESS buffer [33] overnight, and subsequently the tissue was blasted off the skeleton using an airbrush [34]. The DESS-tissue slurry was transferred to 2 ml cryotubes and stored at 4°C until transport to the laboratory facilities at the University of Konstanz, Germany, where samples were stored at -20°C prior to DNA extraction.

DNA was extracted using the Qiagen DNeasy Blood & Tissue kit (Qiagen, Hilden, Germany) using a modified protocol for coral tissue [34]. Briefly, coral tissue slurry stored in DESS buffer was centrifuged at 10,000 x *g* for 3 min at room temperature to pellet the tissue slurry, and subsequently the supernatant DESS buffer was decanted. From the slurry, 90 µL were pipetted into a new 2 mL tube and topped up with 90 µL of ATL buffer as well as 20 µL Proteinase K to make up a total volume of 200 µL. The mixture was vortexed and incubated at 56°C for at least two and up to six hours, depending on the sample, to fully lyse the tissue. After adding 4 µL of RNase A and incubating the sample for 2 mins at room temperature, the manufacturer's protocol was followed. The elution volume was 30 µL for all samples. DNA quantity and quality were assessed with a NanoDrop2000 (Thermo Fisher Scientific, Waltham, Massachusetts, USA) spectrophotometer. Several samples had to be re-extracted due to low DNA concentrations and in the cases where two elutions existed, both were pooled for downstream applications. Extracted DNA was sent to the NGS Competence Center Tübingen (NCCT) for library preparation using the NEBNext Ultra II DNA Library Prep Kit (New England Biolabs, Massachusetts, USA), PCR amplification with cycles dependent on input material (100 ng input material: 4 cycles; 50 ng input material: 5 cycles; 0–27 ng input material: 9 cycles), and subsequent whole genome shotgun (WGS) sequencing on an Illumina NovaSeq6000 (2 x 155 bp). Libraries were sequenced on two lanes for each sample to minimize lane-specific biases. The resulting sequencing files were merged for downstream analyses.

Read processing, variant calling, and variant filtering

Following Illumina WGS, the Genome Analysis Toolkit (GATK) Best Practices [35] were followed for read processing, variant calling, and variant filtering. Briefly, raw FASTQ files were quality checked using FastQC v0.12.1 [36], then, adapters were removed, and the sequencing files were trimmed using BBDuk from the BBMap v39.08 package [37]. Subsequently, the FASTQ files were aligned to the *Porites harrisoni*

reference genome [31] using BWA MEM v0.7.18 [38]. The mapped reads were sorted and quality filtered for a mapping quality of ≥ 30 using SAMtools v1.21 [39]. Read groups were added to each BAM file using PICARD v3.1.1 [40], and duplicates were marked with Sambamba markdup v1.0.1 [41]. Variants were called using GATK HaplotypeCaller with the *P. harrisoni* genome as reference and output in genomic variant call format (--emit-ref-confidence GVCF). The GVCF files were combined using GATK CombineGVCFs and jointly genotyped using GATK GenotypeGVCFs. The resulting VCF file was filtered for SNPs using GATK SelectVariants, and sites were excluded using GATK VariantFiltration using the following flags: low quality by depth score (QD < 2), high Fisher strand score (FS > 60), low mapping quality (MQ < 40), low read position rank sum score (ReadPosRankSum < − 8), high strand odds ratio (SOR > 4), low mapping quality rank sum score (MQRankSum < − 12.5), and depth filtering based on sample size (DP < 2; DP > 238). The SNPs were then filtered using VCFtools v0.1.16 [42], tailored to the requirements of each downstream analysis (see below).

For population structure analyses, SNPs were filtered for minimum quality (--minQ 30), minor allele frequency (MAF) > 0.05 (--maf 0.05), a maximum missing genotype call rate of 20% for each SNP (--max-missing 0.8), Hardy-Weinberg equilibrium (--hwe 0.001), linkage disequilibrium (SNPs in approximate linkage equilibrium were pruned using a window size of 200 bp and an r^2 threshold of 0.2), and only bi-allelic SNPs were retained (--min-alleles 2, --max-alleles 2). Lastly, samples with more than 30% missingness (--mind 0.3) were removed, since a threshold of 20% greatly reduced the number of samples in the AA population, while population structure analyses with both thresholds yielded qualitatively consistent population genetic patterns. This resulted in the removal of 25 samples (*n* = 10 from SA, *n* = 0 from SY, and *n* = 17 from AA). For the selective sweep analyses, SNPs were filtered using the following flags: --minQ 30, --max-missing 0.8, --min-alleles 2, --max-alleles 2, --mind 0.2, linkage disequilibrium (window size 200 bp, r^2 < 0.2) and --maf 0.002, because alleles driven to or near fixation or loss are often present at extreme frequencies (at or close to 1 or 0), and excluding low-frequency variants would risk discarding true signals of selection. A MAF threshold of 0.002 ensured capturing these true signals while filtering out spurious elements.

Clone mate identification and removal

To evaluate kinship across all colonies and remove clones from the resulting VCF files used in the population structure and selective sweep analyses, the program KING v2.2.7 [43] was run on the VCF file filtered for population structure analyses (see above). A kinship coefficient of 0.354 is the geometric mean of first-degree kin (i.e., full siblings; 0.25) and twins (0.5), and is used as the cut-off for distinguishing the two levels of relatedness [43]. Therefore, samples with a kinship coefficient of > 0.354 were assigned as clone mates and the individual with the least amount of genotype missingness was retained for downstream analyses in both VCF files (for population structure and selective sweep analyses, respectively).

Population structure

We assessed population structure among our samples using principal component analysis (PCA) and maximum likelihood estimation of individual ancestries using the program ADMIXTURE [44] using the filtered VCF file for population structure (see above). PCA was performed in PLINK v1.90 [45], and the eigenvectors and eigenvalues were imported into R for plotting. To assess whether specific SNPs contributed disproportionately to the clustering pattern observed at the sites SA and SY, 10,000 SNPs were randomly resampled across 20 replicates of the whole dataset and plotted as before. To prepare input data for ADMIXTURE, the VCF file was converted to a BED file using PLINK v1.90. Then, ADMIXTURE was run from $K = 1$ to $K = 10$ with 10 iterations for each run using altering random seeds. The cross-validation error was calculated from the output and plotted in R. The clusters output by the independent runs for each K were permuted using CLUMPP [46] to find the most probable assignment for each cluster. CLUMPP output files were plotted in R using the package pophelper v2.3.1 [47]. To assess the level of population genetic differentiation present between the three sampling locations, we calculated pairwise Weir & Cockerham's F_{ST} [48] in VCFtools v0.1.16. Lastly, to estimate historical changes in effective population size of *P. harrisoni* populations in the southern PAG, we used Stairway Plot v2 [49]. Briefly, genotype likelihoods from sites SA and SY ($n = 79$) were calculated in ANGSD v0.94 [50] from the BAM files of each sample, and the site frequency spectrum was subsequently estimated from the genotype likelihoods using the module realSFS. To be able to accurately date historic changes in effective population size, a per generation mutation rate of 4.69×10^{-8} per nucleotide site was used based on inferred per year mutation rates for *Porites* corals [51,52] as well as a generation time of 34 years [53]. The output of Stairway Plot v2 was plotted with the ggplot2 v3.4.2 package in R [54].

Host-symbiont genotype-genotype association

For host-symbiont genotype-genotype association analyses, since retaining all clonal host colonies allows for a complete representation of within-host genotypic variation and comparison to symbiont genetic diversity, the filtered VCF file used for population structure analyses (see above) including all clone mates (i.e., before clone mate removal) was taken as input. A hierarchical clustering dendrogram based on identity-by-state (IBS) values calculated in PLINK v1.90 was constructed with hclust() in the stats v4.1.3 package in R [55]. Symbiont assemblage data (i.e., relative abundance of predicted ITS2 type profiles for each coral colony) as output by SymPortal [56] from a published dataset was used [21] (the run can be accessed at https://symportal.org/data_explorer/?Study=202307_afiesinger_UAE_GS). PCA was performed in PLINK v1.90, the eigenvectors and eigenvalues were imported into R for plotting, and each colony was colored or faceted by majority ITS2 type profile assignment (i.e., > 50% relative abundance). To test the association between host and algal symbiont genetic distance, Mantel tests were conducted between host genetic distance calculated from the VCF file and Bray-Curtis non-square-root transformed between sample distance matrices for 'defining intragenomic variants' (DIVs) contributing to ITS2 type profiles from each algal symbiont genus (*Symbiodinium*, *Cladocopium*, *Durusdinium*) output by SymPortal

[56]. The VCF file was loaded into R using the vcfR v1.15.0 package and Mantel tests were calculated with 9,999 permutations for each test using the vegan v2.7.2 package in R [57,58].

Candidate regions of selection

We searched for signatures of selection utilizing genetic differentiation and haplotype homozygosity measures using the filtered VCF file for selective sweep analyses (see above). To quantify genomic divergence between PAG (sites SA and SY) and GO (site AA) *Porites harrisoni*, we computed pairwise Weir and Cockerham's F_{ST} along the genome with VCFtools v0.1.16. To calculate haplotype homozygosity statistics, genotypes were first phased and imputed in Beagle v5.5 [59,60]. Then, cross-population extended haplotype homozygosity (XP-EHH) [61], integrated haplotype score (iHS) [62], number of segregating sites by length (nSL) [63], and integrated haplotype homozygosity pooled (iHH12) [64] were calculated using selscan v2.1 [65,66] and normalized to account for genome-wide differences in haplotype length between the PAG and GO using the selscan normalization script [66]. SNPs were considered outliers (i.e., in candidate regions of selection) if two conditions were met: (i) they were in the top 0.1% quantile of F_{ST} values and (ii) the absolute XP-EHH score was in the top 1% tail of the statistic (corresponding to an absolute XP-EHH ≥ 3.09) and positive, reflecting the presence of extended haplotypes (indicative of selective sweeps) in the PAG corals compared to the GO. Candidate loci identified through both the F_{ST} and XP-EHH outlier analysis, were analyzed with SnpEff v5.3 [67] to annotate and predict the effects of genetic variants (e.g., amino acid change in the coding sequence of a gene) based on the *P. harrisoni* reference genome, and the results were filtered using SnpSift v5.3 [68]. For each identified candidate region, allele frequency was calculated with VCFtools v0.1.16 and plotted in R to determine whether alleles in the respective regions were at or near fixation in the PAG corals. Further, linkage disequilibrium decay was assessed using PopLDDecay v3.40 [69] on the population structure VCF file before LD pruning (--minQ 30, --maf 0.05, --max-missing 0.8, --hwe 0.001, --min-alleles 2, --max-alleles 2). Lastly, to identify regions where loss in nucleotide diversity (π) could be observed in the PAG but not the GO or vice versa (indicative of directional selection), π was calculated on the VCF file output by GATK with an additional flag to include all variant sites (--include-non-variant-sites). Clone mates were removed as above, and π was calculated with pixy [70].

Results

To shed light on population genetic structure and signatures of selection of *Porites harrisoni* in the southern Persian/Arabian Gulf (PAG) in comparison to the environmentally more benign Gulf of Oman (GO), we sampled a total of 119 *P. harrisoni* colonies from two sites in the PAG (n = 40 at site SA, n = 39 at site SY) and one site in the GO (n = 40 at site AA; Fig. 1a). The maximum monthly mean (MMM) climatology shows that the southern PAG sites are thermally more extreme than the neighboring GO site (MMM = 32.6°C at AA), with MMM values of 34.1°C at SA and 33.9°C at SY. Furthermore, the southern PAG experiences large seasonal temperature variations (< 20°C in winter months, > 35°C in summer

months), whereas the GO is exposed to lesser variation and temperature extremes, with temperatures of < 25°C in winter and > 30°C in summer [3,9]. Illumina whole genome shotgun (WGS) sequencing of all sampled colonies yielded a mean coverage of 45X (6–68X per sample). After variant calling following the Genome Analysis Toolkit (GATK) Best Practices, the resulting VCF file was subjected to analysis-specific filtering and clone mate identification through kinship analysis, which prompted the removal of two samples, one from site SA and one from site AA (Supplementary Figure S1).

Population genetic structure of Porites harrisoni *in the PAG and GO*

To assess the population structure of *Porites harrisoni* across the southern PAG and the adjacent GO, we estimated pairwise genetic differentiation (Weir & Cockerham's F_{ST}), performed principal component analysis (PCA), and conducted model-based clustering using ADMIXTURE (Fig. 1). The filtered VCF file for population structure analyses (--maf 0.05, --max-missing 0.8, --mind 0.3, --hwe 0.001, --ld-r2 0.2) yielded a total of 663,850 SNPs in 92 samples (25 samples were removed due to a high amount of missingness, see Methods). Genetic differentiation among populations was low overall, yet spatial patterns were present. Pairwise F_{ST} was lowest among the two southern PAG sites (SA vs. SY: F_{ST} = 0.021) and increased with increasing physical distance between each site (SY vs. AA: F_{ST} = 0.027; SA vs. AA: F_{ST} = 0.041) (Fig. 1a inset). Thus, genetic divergence increased with geographic distance and across the Strait of Hormuz connecting the PAG and GO. This notion was supported by the PCA (Fig. 1b), which showed that SA and SY formed distinct clusters, with some SY colonies forming clusters among the more dispersed AA colonies. By comparison, the higher spread among AA colonies suggests broader genetic variation among GO colonies. The first two principal components explained 11.22% and 8.92% of the variance, respectively, with individuals from all three sites showing overlap in PCA space, suggesting overall limited genetic differentiation (Fig. 1b). To assess whether specific SNPs contributed overproportionately to the clustering pattern observed in SA and SY, 10,000 SNPs were randomly resampled across 20 replicates. The resulting PCAs exhibited patterns consistent with those obtained from the complete dataset, arguing for a homogenous contribution of many SNPs to the observed pattern (Supplementary Figure S2).

ADMIXTURE analyses revealed that PAG corals share an ancestral population that is distinct from the GO (Fig. 1c). Across ten independent runs from K = 1 to K = 10, cross-validation identified K = 1 and K = 2 as the best-supported models. As K = 1 does not separate the samples into different clusters and values of $K \geq 5$ showed high cross-validation errors (Fig. 1c inset), they were not considered to be suitable models. At K = 2, the two clusters separated the samples into subpopulations corresponding to their locations, with colonies from the PAG (SA and SY) predominantly assigned to one cluster, while colonies from the GO (AA) showed markedly mixed ancestry proportions with only a few colonies clearly assigned to the other cluster (Fig. 1c). At higher values (K = 3 and K = 4) no clear partitioning was apparent and ancestry was mixed, supporting K = 2 to be best suited to resolve the ancestry proportions observed in these three sampled locations. The results indicate that gene flow between the PAG and GO is present, but that certain barriers to gene flow exist, with SA showing almost no signs of admixture.

Due to the young age of the PAG (approx. 6k years) [15], likely only a few populations have colonized the PAG during its expansion in the Holocene. A stairway plot based on the site frequency spectrum of the two PAG sites (SA and SY, *n* = 79) revealed a pronounced and recent decline in effective population size (N_e) in *Porites harrisoni* (Supplementary Figure S3). The results show historically large N_e values, which fell sharply around 10-20k years ago, in line with the first shoreline expansions of the PAG, and another decline when the present-day PAG shorelines were established approx. 6k years ago [71] with a more modest decline below 10k individuals up until today, suggesting a founder effect or a population bottleneck. Taken together, these findings indicate that overall genetic differentiation among the three sites remains low, albeit the separation of SA in the PCA and clustering analysis suggest that certain barriers to gene flow and larval exchange exist in the southernmost site of the PAG.

Host genotype and environment contribute to algal symbiont assemblages

To elucidate the relationship between host genetic diversity and associated algal symbiont assemblage in *Porites harrisoni*, we assessed whether host genetic distance correlated with the identity of the dominant (i.e., > 50% relative abundance) ITS2 type profile (algal proxy-genotypes), retaining host clone mates in the analysis. Coral host kinship analysis using KING revealed two sets of clone mates with two individuals each, which were confirmed through hierarchical clustering based on pairwise identity-by-state (IBS) values calculated in PLINK (Fig. 2a).

The first set of clone mates from the site SA hosted two related, but distinct ITS2 type profiles (C3-C3gulf-C3cc and C3-C3cc-C3gulf-C3ye, both belonging to the species *Cladocopium thermophilum*) [72], while the second set of clone mates from the site AA shared an identical ITS2 type profile (D1/D4-D4c-D1h, belonging to the species *Durusdinium trenchii*) [73]. Each of the ITS2 type profiles were present at 100% relative abundance within their respective host colony (i.e., no background symbionts). Overall, host genetic similarity did not strictly correlate with algal symbiont ITS2 type profiles, since we found shared ITS2 type profiles across genetically differentiated host genotypes. Nonetheless, host colonies with greater genetic similarity also tended to host more closely related ITS2 type profiles, which was observed for all three algal species (i.e., *Cladocopium thermophilum, Durusdinium trenchii*, and *Symbiodinium microadriaticum*). In addition, ITS2 type profile identity also reflected geographic location, i.e., colonies at SA and SY predominantly hosted genotypes of *C. thermophilum*, while colonies at AA hosted mainly *D. trenchii* and *S. microadriaticum* genotypes (Fig. 2b,c). Mantel tests assessing the correlation between host and symbiont pairwise genetic distance revealed a moderate and significant association for *Cladocopium* (r = 0.2387, p = 0.01), a moderate, yet non-significant association for *Durusdinium* (r = 0.2516, p = 0.0556) and a weak and non-significant association for *Symbiodinium* (r = 0.05773, p = 0.2447). Taken together, these results argue that the environment and the host contribute to symbiont association/specificity, with a stronger contribution of host identity for *Cladocopium* ITS2 type profiles. Albeit subject to further exploration, these findings provide the first indication of genotype-level

specificity in algal symbionts in *P. harrisoni*, in addition to a role of the environment shaping symbiont assemblages [17,21].

Candidate regions under positive selection

To identify candidate regions under putative positive selection in *Porites harrisoni*, we tested for differentiated SNPs between the PAG and GO using Weir & Cockerham's F_{ST} and compared these with genomic regions exhibiting high cross-population extended haplotype homozygosity (XP-EHH). After sweep analysis-specific filtering of the VCF file (--maf 0.002, --max-missing 0.8, --mind 0.2, --ld-r2 0.2), a total of 2,878,739 SNPs in 81 samples were retained (*n* = 24 from SA, *n* = 39 from SY, and *n* = 18 from AA). The *P. harrisoni* reference genome [31] is 626 Mb in size, therefore rendering a SNP density of ~ 4.59 SNP per kb for this dataset. We identified a total of 394 common outlier SNPs in both approaches (Supplementary Figure S4), and subsequently identified two contigs containing the highest values of F_{ST} and XP-EHH as candidate regions under positive selection (Fig. 3).

On contig 29 (total length 2.0 Mb, *n* = 67 genes of which 22 are annotated), F_{ST} values between the PAG and GO populations were the highest found along the genome (up to 0.93; Fig. 3a,b). In the corresponding genomic region of contig 29 (640 Kb in length, *n* = 18 genes of which 6 are annotated), haplotypes were longer in the PAG compared to the GO (normalized XP-EHH scores up to 7.37; mean contig 29-wide XP-EHH = 0.45; mean genome-wide XP-EHH = 6.37×10^{-10}). In this candidate region of selection, SnpEff analysis showed that 40 of 50 common outlier SNPs were located in intronic regions, 2 in intergenic regions, 5 up- or downstream of a gene, 1 in a 3' untranslated region (UTR), and 2 in coding sequences (CDS; Supplementary Table S1). Of the CDS variants, one was predicted to cause a synonymous codon change to an unannotated protein (GeneID g3852) with a low predicted impact, while the other variant was predicted to cause a nonsynonymous change to an unannotated protein (GeneID g3839) with a moderate predicted impact. Gene annotation was based on the *P. harrisoni* reference genome [31]. Of the six annotated genes, COL4A1 and COL2A1 (collagen type IV alpha 1 and collagen alpha-1(II) chain, respectively) are important proteins of the basement membrane (a specialized form of the extracellular matrix; ECM), essential for tissue architecture and function [74,75]. In *Acropora palmata* and *Acropora hyacinthus*, ECM remodeling (including collagens) was up-regulated during thermal stress, suggesting a role in thermal resilience [76,77]. ACVR2B (activin receptor type-2B) and BMPR2 (bone morphogenetic protein receptor type-2) are members of the transforming growth factor-β (TGF-β) superfamily [78,79]. In corals and other cnidarians, both genes are potentially relevant for thermal tolerance through immune modulation and the TGF-β/activin pathways that regulate apoptosis and cell survival. In *Orbicella faveolata* TGF-β likely contributes to immune regulation [80], and in *Aiptasia pallida* it may contribute to host control over algal symbiont populations [81], critical under heat stress. ORC4 (origin recognition complex subunit 4) is part of a conserved eukaryotic initiator directing DNA replication [82]. Lastly, CDK2 (cyclin-dependent kinase 2) is a necessary activator for passage through the cell cycle in eukaryotes [83] and was found to be under positive selection in *Platygyra daedalea* in PAG corals [18]. Thus,

genes within the putative region of positive selection have previously been implicated in the heat tolerance of corals.

On contig 62 (total length 1.5 Mb, *n* = 63 genes of which 25 are annotated), normalized XP-EHH values reached up to 10.47 (mean contig 62-wide XP-EHH = 1.63; mean genome-wide XP-EHH = 6.37×10^{-10}), indicating regions of extended haplotype homozygosity on this contig for the PAG corals (Fig. 3a,c). Within the corresponding genomic region (spanning 526 Kb), F_{ST} values were as high as 0.69 and a total of 17 annotated genes (of a total of 36 genes) were found with a variety of functions (Fig. 3c). Out of a total of 49 common outlier SNPs, SnpEff analysis identified 13 SNPs located in intronic regions, 23 in intergenic regions, 2 up- or downstream of a gene, 3 in 3' and 1 in 5' UTR, and 7 in CDS (Supplementary Table S2). Of the 7 variants in CDS, 5 were predicted to cause a synonymous codon change within the genes PDCD6, KDELC1, ANO10, and eva-1 with low predicted impact. The other two variants were predicted to cause nonsynonymous codon changes to TTLL9 and eva-1 with a moderate impact. TTLL9 is a putative tubulin polyglutamylase and eva-1 is a SUEL-type lectin domain-containing protein. Lectins assumingly play a role in the recognition of the coral-algal symbiosis in *Fungia scutaria* [84] and tubulin proteins are presumably involved in the coral host immune system. For example, TUBB4B (tubulin beta-4B chain) was shown to be up-regulated in *O. faveolata* during a bleaching event [85]. The gene PDCD6 (programmed cell death protein 6) is implicated in the innate immune response and plays roles in regulating apoptosis, alternative splicing, and cytoskeletal integrity [86]. KDELC1 (protein O-glucosyltransferase) is involved in the stress response of the endoplasmic reticulum [87]. This gene was found to be up-regulated in corals exposed to heat stress, indicating a potential role in thermal resilience [88]. The gene ANO10 (anoctamin 10) has a role in controlling the contractions underlying tentacle pulsation of cnidarians such as *Hydra* [89] and the octocoral *Xenia umbellata* [90]. ANKS6 (ankyrin repeat and SAM domain-containing protein 6) and RSPH10B (cadherin member 2) are genes from the 'membrane-binding' domain [91,92]. PDRG1 (p53 and DNA damage-regulated protein 1) has functions associated with cell proliferation, growth, apoptosis, cell cycle regulation, and DNA damage repair [93]. DYNC1LI1 (cytoplasmic dynein 1 light intermediate chain 1), RAB22A (ras-related protein Rab-22A) and DCAF11 (DDB1- and CUL4-associated factor 11) are genes involved in intracellular processes. DYNC1LI1 is implicated in intracellular trafficking and chromosome segregation during mitosis [94], RAB22A is a key organizer of intracellular membrane transport [95], and DCAF11 is implicated in the regulation of transcription and protein degradation as an E3 ligase capable of supporting ligand-induced protein degradation [96]. RBM18 (putative RNA-binding protein 18) is an RNA-binding protein, essential for various aspects of gene expression, including alternative splicing [97]. The latter was shown to be increased in response to heat stress in *Acropora cervicornis*, potentially representing an important regulatory mechanism for thermal stress response in corals [98]. FBXO31 (F-box only protein 31) is a protein involved in the Ubiquitin-mediated proteolysis, which in turn is involved in protein degradation and turnover [99]. F-box genes have been found to be upregulated in heat stressed corals [100,101]. Other genes found in this region are HNF4A (hepatocyte nuclear factor 4-alpha), ZDHHC7 (palmitoyltransferase), and SSNA1 (Sjoegren syndrome nuclear autoantigen 1). Collectively, these results identify a large, highly

differentiated genomic region in PAG corals characterized by extended haplotypes and enriched for genes involved in immune function, cellular stress responses, and intracellular regulation, consistent with a target of positive selection that is potentially contributing to thermal adaptation.

Aside from the nature of the identified genes, it is remarkable to note that allele frequency plots confirmed almost invariant SNPs in both candidate regions in PAG colonies, but not in GO corals (Supplementary Figure S5). While nucleotide diversity was not widely reduced in the PAG compared to the GO on contigs 29 and 62 (Supplementary Figure S6; which could point to a hard selective sweep, if present), the H-statistics (integrated haplotype score; iHS, number of segregating sites by length; nSL, and integrated haplotype homozygosity pooled; iHH12) showed expansion in the identified candidate regions (Supplementary Figures S7 and S8), with the highest absolute values of iHH12 and nSL found on contig 62 (iHH12 = 8.47, |nSL| = 5.15). These results may suggest soft rather than hard selective sweeps in the identified genomic regions. Genome-wide patterns of linkage disequilibrium (LD) decay showed that PAG haplotypes decayed at a slower rate (i.e., were longer) than those of the GO, in line with the identification of selective sweeps in PAG but not GO corals (Supplementary Figure S9).

Discussion

The coral *Porites harrisoni* is a common reef builder in the Arabian Seas with an exceptional heat tolerance, making it able to survive in the thermally extreme and highly saline environment of the southern PAG [5,11,14]. This environment assumingly imposes strong directional selection, likely shaping the genomic architecture of resident corals [18,24]. Accordingly, *P. harrisoni* could provide critical insight into the genomic basis of coral thermal tolerance under a warming climate. As one of the last remaining stony corals in the region [8], research on this species is critical to inform potential genetic rescue efforts, such as assisted gene flow, i.e., the movement of standing genetic variation from one population to another to increase the recipient population's adaptive potential, e.g., by means of selective breeding [24,25,102]. Here, we characterized the population genetic structure of *Porites harrisoni* across the PAG and GO to assess the extent of their divergence. This also enabled us to examine the specificity of host–algal symbioses at the level of coral genotypes and algal ITS2 type profiles, which are thought to underpin the exceptional thermal tolerance of PAG corals [5,10,17,21,103]. Finally, we investigated signatures of selection to identify genomic regions and genes potentially associated with adaptation to the extreme environment of the PAG.

Previous work utilizing biophysical models suggests that coral populations in the PAG could become more isolated with ongoing ocean warming [104]. Therefore, studying the genetic connectivity of prevalent reef-builders in the PAG is important to predict their responses to ongoing climate change. While studies on *Platygyra daedalea* exist, the population genetic structure of southern PAG *P. harrisoni* is not documented to date [18,105]. Based on our analyses, the low overall genetic differentiation among *P. harrisoni* across the three sampling sites indicates a high degree of genetic connectivity of PAG colonies across the Strait of Hormuz with the neighboring GO, with differentiation increasing with distance

(Fig. 1). To determine ancestry proportions, ADMIXTURE was run from *K* = 1 to *K* = 10, and *K* = 2 was identified as the best suited model. At *K* = 2, our results show that gene flow is present but certain barriers exist that potentially isolate the southernmost site, SA. Our results further indicate that the PAG populations trace back to an ancestral lineage that is distinct from that of the GO. This is consistent with the oceanographic conditions in the PAG, where surface waters from the GO enter the PAG through the Strait of Hormuz and move counterclockwise toward the southern basin [9,106]. Such currents likely facilitate larval dispersal and genetic exchange from the GO into the PAG as well as within the PAG, while restricting outward connectivity towards the GO. This pattern corroborates previous findings in *Platygyra daedalea* [18], where southern PAG *P. daedalea* populations were predominantly composed of one genetic cluster and GO populations of another. Demographic reconstructions revealed pronounced reductions in effective population size coinciding with the Holocene establishment of the modern PAG [15], suggesting a founder effect or population bottleneck as corals colonized this young ocean basin (approx. 6ka years ago) [15,16]. The limited time available for post-glacial colonization emphasizes the role of positive selection acting on standing genetic variation in the founder population, rather than on adaptive mutations arising since the PAG was colonized, as shown for the evolutionary history of *C. thermophilum* in the PAG [17]. The strong selective pressures of this extreme habitat likely acted on the available standing genetic variation, promoting the retention and/or rapid adaptation of thermally resilient genotypes [17].

To explore levels of host-algal specificity, we mapped host genotypes onto ITS2 type profiles (as proxies for algal genotypes) [56] for each coral colony of *P. harrisoni*. This study, in line with a previous study [21], shows that genetically identical hosts can harbor different symbiont assemblages based on ITS2 type profiles (Fig. 2), pointing to environmental heterogeneity as a driver of symbiont association even within sites. Nonetheless, genus-separated Mantel tests between host and algal genetic distances revealed a moderate but significant association for *Cladocopium*, while the association was non-significant and weak (for *Symbiodinium*) to moderate (for *Durusdinium*) for the other two genera. Coral hosts from the PAG were almost exclusively associated with *Cladocopium thermophilum*, while colonies from the GO were predominantly associated with *Symbiodinium microadriaticum* and *Durusdinium trenchii*. Given the presumed vertical transmission mode of algal symbionts in *P. harrisoni* [10,105], the geographical variation in clonal colonies hosting the same (in the GO) and distinct (in the PAG) ITS2 type profiles potentially reflects environmentally driven differential retention or loss of maternally inherited symbionts. Together, these results indicate that both environment and host identity shape algal symbiont assemblage [107–109]. Overall, the host–algal symbiosis in PAG corals appears increasingly constrained, with a reduced diversity of *Cladocopium thermophilum* genotypes observed over the past decade [21]. Given that symbiont genotype affects host thermal tolerance and bleaching outcomes, this narrowing likely restricts both ecological flexibility and evolutionary potential of the coral holobiont [5]. This suggests that an environment becoming even more extreme under accelerating climate change will impose more constraints on the availability of heat-adapted symbionts to sustain their coral holobionts. Thus,

although PAG corals are among the most heat-tolerant corals globally, the narrowing pool of suitable symbionts may render them increasingly susceptible to extreme and recurrent thermal stress [102].

Genomic analyses for signatures of selection revealed localized regions of pronounced differentiation in PAG corals. The identification of two genomic regions exhibiting strong genetic differentiation and cross-population extended haplotype homozygosity demonstrates clear and specific signatures of positive selection distinguishing PAG from GO colonies (Fig. 3). Moreover, the presence of highly differentiated and nearly fixed SNPs in PAG corals suggests the presence of what one may consider 'non-negotiable SNPs'. These are specific alleles that assumingly must be present in genotypes to persist under the harsh conditions in the PAG. In this instance, the exceptionally high F_{ST} (up to 0.93) and XP-EHH values (normalized scores up to 7.37) on contig 29 (Fig. 3b) indicate a localized selective sweep in the PAG, with several genes in this region linked to ECM remodeling, apoptotic regulation, and cell-cycle control – processes known to contribute to thermal resilience in corals [18,76,77,110]. The finding of highly differentiated SNPs against a backdrop of a low population-wide F_{ST} underscore unusually strong selective pressures on this specific region, strongly implying essential adaptive functions for coping with the prevailing environment. Such a strong signal of selection was not found in *Platygyra daedalea* in the PAG [18], albeit that study presented evidence for a hard selective sweep, with high differentiation, extended haplotypes, and a reduction in nucleotide diversity, which was not found in our study (Supplementary Figure S6). Different from the exceptionally high F_{ST} for contig 29, we detected extraordinarily long haplotypes on contig 62 (normalized XP-EHH values up to 10.47) in conjunction with strong differentiation (F_{ST} up to 0.69; Fig. 3c). Under further consideration of the elevated iHH12 and nSL values (Supplementary Figure S8), this points to strong selection affecting a broad genomic interval. The corresponding region on contig 62 is enriched for genes associated with immune regulation, intracellular trafficking, ER stress response, and RNA processing – pathways that are repeatedly implicated in coral thermal tolerance [85,88,98].

The presence of multiple outlier SNPs in non-coding regions, synonymous mutations, and the distribution of variants across intronic and intergenic regions suggests that regulatory mechanisms may be a primary target of selection rather than coding sequence changes per se as key drivers of adaptation in extreme environments. Allele frequency patterns showing near fixation in PAG colonies, but not in GO corals, reinforce that selective pressures specific to the PAG environment have shaped these genomic regions (Supplementary Figure S5). Notably, the absence of pronounced reductions in nucleotide diversity suggests a soft sweep (Supplementary Figure S6), implying that selection acted on multiple alleles present in the ancestral standing variation, rather than on a single novel mutation. Extended linkage disequilibrium observed in PAG corals confirms more extensive haplotype structure, consistent with selection on linked loci in these extreme habitats (Supplementary Figure S9). A total of 23 annotated genes were found in both regions under positive selection with a variety of functions in response to heat stress and a challenging environment, e.g., processes involving innate immunity, cytoskeletal activity, membrane organization, the cell-cycle, protein turnover, and gene expression. Of note are genes implicated in apoptosis and host–algal symbiosis such as PDCD6 and ACVR2B. Under

heat stress, fine-scale modulation of apoptosis is central to mediating symbiont retention or loss, a pattern observed in *Porites astreoides* in a highly variable environment in the Florida Keys, where a dynamic expression response was observed in genes implicated in symbiont retention [111]. Combined with reports of heat-induced alternative splicing [98], this points to these genes acting as pathways connecting apoptosis control, protein turnover, and thermal resilience. Host control over symbionts may sustain the crucial symbiosis, especially with *Cladocopium thermophilum* genotypes in the southernmost basin of the PAG. Collectively, the variety of gene functions support a multifaceted genomic architecture underlying stress responses, host–symbiont dynamics, and cellular homeostasis in PAG corals exposed to extreme temperatures.

Porites harrisoni in the PAG has one of the highest ecological bleaching thresholds in the world [5,15]. However, it also lives perilously close to its upper thermal tolerance threshold [5]. Despite their remarkable persistence, the declines across PAG coral assemblages in recent decades underscore that coral thermal tolerance is ultimately constrained [8,25,112]. The reductions in coral cover observed in this thermally extreme region in recent years have substantially diminished the pool of reproductively capable coral colonies, while bleaching-related physiological impairment has likely reduced fecundity in at least some taxa, thereby lowering reproductive output [8,12,113]. Moreover, extensive bleaching of offshore reefs and those in neighboring water bodies since 2017 suggests that demographic rescue via larval influx from distant source populations is unlikely [114], conveying the need for a public discussion about active intervention strategies [30,115,116]. In this context, consideration of adaptive haplotypes identified through genomic studies could inform strategies such as genetic rescue [24,26,27,29]; however, such approaches must be tempered by recognition of the limits imposed by continuing warming that may surpass even the thermal tolerance of PAG corals. Moreover, active intervention methods must consider the constraints imposed by the high salinity levels in the southern PAG, whereby the exceptional thermal tolerance of PAG corals is diminished when they are exposed to more conventional salinity levels [16]. In this context, selectively bred larvae from PAG populations introduced into the cooler regime of the GO may not survive in the long term [24]. This in turn warrants further studies into the applicability of these approaches and the role of salinity in conveying thermal tolerance [117,118].

In such an extreme habitat, the suite of viable adaptive paths is inherently constrained. Severe and persistent temperature and salinity stress impose a narrow selective regime under which only a limited number of allelic variants confer survival. The strong selective environmental filtering potentially narrows the range of viable genotypes and constrains future adaptive capacity [5], which may limit the long-term persistence of these coral populations. The pronounced differentiation of a small subset of SNPs is consistent with this scenario. The host–algal symbiosis and genomic adaptations of *P. harrisoni* have likely been shaped over millennia, whereas future adaptation to accelerating ocean warming would need to occur over decades. Whether such rates of adaptation are achievable in long-lived reef-building corals remains uncertain. Climate mitigation strategies at a regional and global scale are therefore more important than ever.

Declarations

Competing interests

The authors declare no competing interests.

Funding

AF and CRV were supported by the Deutsche Forschungsgemeinschaft (DFG, German Research Foundation) under project number 433042944 (https://gepris.dfg.de/gepris/projekt/433042944?language=en), and LC and CRV were supported by the DFG under project number 458901010 (https://gepris.dfg.de/gepris/projekt/458901010?language=en). LKB, SG, NSB, JJV, DJB, IBB, RA, and CRV were supported by the Paul G. Allen Family Foundation project 'Global Search for Genetic Regulators of Coral Resilience to Thermal Stress' (G-12948). JAB was supported by funding from Tamkeen under the NYUAD Research Institute grant CG009 to Mubadala ACCESS and grant CGSB5 to CGSB.

Author contributions

CRV conceived and conceptualized the study. AF, CRV, GP, HM, RA collected samples. JAB provided field support. CRV, DJB, IBB, JJV, LKB, and NSB provided funding. AF conducted molecular extractions, data analysis and visualized the results with contributions from CRV, LC, and RA. AF and CRV conducted data interpretation and wrote the manuscript. All co-authors reviewed and approved the final manuscript.

Acknowledgements

We kindly thank the NYU Abu Dhabi Core Technology Marine Science group and particularly Dain McParland for field support and his help in collection of coral samples. We thank Sarah W. Davies for her supervision of the doctoral thesis of AF and her valuable comments on the manuscript. We gratefully acknowledge the Environment Agency Abu Dhabi research permit with the reference number 56930. This is publication number 6 of the Global Search Consortium https://zenodo.org/communities/globalsearch/.

Data availability

Raw whole genome sequencing data are available under the NCBI BioProject PRJNA1191362 (https://www.ncbi.nlm.nih.gov/bioproject/PRJNA1191362), nested under the Umbrella Project PRJNA749006 (https://www.ncbi.nlm.nih.gov/bioproject/PRJNA749006). The ITS2 SymPortal run is accessible on SymPortal at https://symportal.org/data_explorer/?Study=202307_afiesinger_UAE_GS.

VCF files generated from raw sequencing data can be accessed at the Zenodo repository [119]. All code for the data analysis and generation of figures is available on GitHub under https://github.com/afiesinger/UAE_PAG_WGS_PopGen_Phar and at the Zenodo repository [120].

References

1. Allen MR et al (2018) „Framing and Context in Global Warming of 1.5 C: An IPCC Special Report on the impacts of global warming of 1.5 C above pre-industrial levels and related global greenhouse gas emission pathways, in the context of strengthening the global response to the threat of climate change, sustainable development, and efforts to eradicate poverty. Preprint at
2. Calvin K et al (2023) IPCC, : Climate Change 2023: Synthesis Report. Contribution of Working Groups I, II and III to the Sixth Assessment Report of the Intergovernmental Panel on Climate Change [core Writing Team, H. Lee and J. Romero (eds.)]. IPCC, Geneva, Switzerland. (2023) 10.59327/ipcc/ar6-9789291691647
3. Coles SL, Riegl BM (2013) Thermal tolerances of reef corals in the Gulf: a review of the potential for increasing coral survival and adaptation to climate change through assisted translocation. Mar Pollut Bull 72:323–332
4. Baker AC, Glynn PW, Riegl B (2008) Climate change and coral reef bleaching: An ecological assessment of long-term impacts, recovery trends and future outlook. Estuar Coast Shelf Sci 80:435–471
5. Alderdice R et al (2025) Summer temperature maxima already challenge thermal capacities of coral in the Southern Persian/Arabian Gulf. 10.21203/rs.3.rs-8231598/v1. Research Square
6. Reimer JD et al (2024) The Fourth Global Coral Bleaching Event: Where do we go from here? Coral Reefs 43:1121–1125
7. Carpenter KE et al (2008) One-third of reef-building corals face elevated extinction risk from climate change and local impacts. Science 321:560–563
8. Burt JA (2024) Coral reefs of the Emirates. A Natural History of the Emirates 325–351. Springer Nature Switzerland, Cham. doi:10.1007/978-3-031-37397-8_11.
9. Yao F, Johns WE (2010) A HYCOM modeling study of the Persian Gulf: 1. Model configurations and surface circulation. J Phys Res
10. Howells EJ, Abrego D, Meyer E, Kirk NL, Burt JA (2016) Host adaptation and unexpected symbiont partners enable reef-building corals to tolerate extreme temperatures. Glob Chang Biol 22:2702–2714
11. Riegl BM, Purkis SJ, Al-Cibahy AS, Abdel-Moati MA (2011) Hoegh-Guldberg, O. Present limits to heat-adaptability in corals and population-level responses to climate extremes. PLoS ONE 6:e24802
12. Burt JA, Paparella F, Al-Mansoori N, Al-Mansoori A, Al-Jailani H (2019) Causes and consequences of the 2017 coral bleaching event in the southern Persian/Arabian Gulf. Coral Reefs 38:567–589

13. Manzello DP et al (2025) Heat-driven functional extinction of Caribbean Acropora corals from Florida's Coral Reef. Science 390:361–366
14. John VC, Coles SL, Abozed AI (1990) Seasonal cycles of temperature, salinity and water masses of the Western Arabian Gulf. Oceanol Acta 13
15. Riegl BM, Purkis SJ (2012) Coral reefs of the gulf: Adaptation to climatic extremes in the world's hottest sea. Coral Reefs of the World 1–4. Springer Netherlands, Dordrecht. doi:10.1007/978-94-007-3008-3_1.
16. D'Angelo C et al (2015) Local adaptation constrains the distribution potential of heat-tolerant Symbiodinium from the Persian/Arabian Gulf. ISME J 9:2551–2560
17. Hume BCC et al (2016) Ancestral genetic diversity associated with the rapid spread of stress-tolerant coral symbionts in response to Holocene climate change. Proc. Natl. Acad. Sci. U. S. A. 113, 4416–4421
18. Smith EG et al (2022) Signatures of selection underpinning rapid coral adaptation to the world's warmest reefs. Sci Adv 8:eabl7287
19. Coles SL (2003) Coral species diversity and environmental factors in the Arabian Gulf and the Gulf of Oman: a comparison to the Indo-Pacific region
20. Hume BCC, D'Angelo C, Burt JA, Wiedenmann J (2018) Fine-scale biogeographical boundary delineation and sub-population resolution in the Symbiodinium thermophilum coral symbiont group from the Persian/Arabian gulf and gulf of Oman. Front Mar Sci 5:343524
21. Fiesinger A et al (2025) Symbiodiniaceae shifts over the last decade on the hottest coral reefs on Earth. Coral Reefs. 10.1007/s00338-025-02767-x
22. Ochsenkühn MA, Röthig T, D'Angelo C, Wiedenmann J, Voolstra CR (2017) The role of floridoside in osmoadaptation of coral-associated algal endosymbionts to high-salinity conditions. Sci Adv 3:e1602047
23. Kirk NL, Howells EJ, Abrego D, Burt JA, Meyer E (2018) Genomic and transcriptomic signals of thermal tolerance in heat-tolerant corals (Platygyra daedalea) of the Arabian/Persian Gulf. Mol Ecol 27:5180–5194
24. Howells EJ et al (2021) Enhancing the heat tolerance of reef-building corals to future warming. Sci Adv 7
25. Humanes A et al (2026) Accelerating coral assisted evolution to keep pace with climate change. Nat Rev Biodivers. 10.1038/s44358-026-00147-z
26. Burt JA et al (2020) Insights from extreme coral reefs in a changing world. Coral Reefs 39:495–507
27. Howells EJ et al (2025) Marine heatwaves select for thermal tolerance in a reef-building coral. Nat Clim Chang 15:829–832
28. Jin YK et al (2016) Genetic markers for antioxidant capacity in a reef-building coral. Sci Adv 2:e1500842

29. Bay RA, Rose NH, Logan CA, Palumbi SR (2017) Genomic models predict successful coral adaptation if future ocean warming rates are reduced. Sci Adv 3:e1701413
30. Voolstra C et al (2021) Extending the natural adaptive capacity of coral holobionts. Nat Rev Earth Environ 2:747–762
31. Fiesinger A et al (2026) The genome of the reef-building coral Porites harrisoni from the southern Persian/Arabian Gulf. GigaByte. (2026)
32. Baums IB, Miller MW, Hellberg ME (2006) GEOGRAPHIC VARIATION IN CLONAL STRUCTURE IN A REEF-BUILDING CARIBBEAN CORAL,ACROPORA PALMATA. Ecol Monogr 76:503–519
33. Yoder M et al (2006) DESS: a versatile solution for preserving morphology and extractable DNA of nematodes. Nematology 8:367–376
34. Voolstra CR et al (2025) DNA preservation & DNA extraction protocol for field collection of coral samples suitable for host-, marker gene-, and metagenomics-based sequencing approaches
35. McKenna A et al (2010) The Genome Analysis Toolkit: a MapReduce framework for analyzing next-generation DNA sequencing data. Genome Res 20:1297–1303
36. Andrews S, FastQC: (2010) A Quality Control Tool for High Throughput Sequence Data
37. Bushnell B (2024) BBMap
38. Li H (2013) Aligning sequence reads, clone sequences and assembly contigs with BWA-MEM. arXiv [q-bio.GN]. 10.48550/ARXIV.1303.3997
39. Danecek P et al (2021) Twelve years of SAMtools and BCFtools. Gigascience 10:giab008
40. Broad Institute. Picard Toolkit, GitHub Repository, Broad Institute (2019)
41. Tarasov A, Vilella AJ, Cuppen E, Nijman IJ, Prins P (2015) Sambamba: fast processing of NGS alignment formats. Bioinformatics 31:2032–2034
42. Danecek P et al (2011) The variant call format and VCFtools. Bioinformatics 27:2156–2158
43. Manichaikul A et al (2010) Robust relationship inference in genome-wide association studies. Bioinformatics 26:2867–2873
44. Alexander DH, Lange K (2011) Enhancements to the ADMIXTURE algorithm for individual ancestry estimation. BMC Bioinformatics 12:246
45. Purcell S et al (2007) PLINK: a tool set for whole-genome association and population-based linkage analyses. Am J Hum Genet 81:559–575
46. Jakobsson M, Rosenberg NA (2007) CLUMPP: a cluster matching and permutation program for dealing with label switching and multimodality in analysis of population structure. Bioinformatics 23:1801–1806
47. Francis RM (2017) pophelper: an R package and web app to analyse and visualize population structure. Mol Ecol Resour 17:27–32
48. Weir BS, Cockerham CC (1984) Estimating F-statistics for the analysis of population structure. Evolution 38:1358

49. Liu X, Fu Y-X (2020) Stairway Plot 2: demographic history inference with folded SNP frequency spectra. Genome Biol 21:280
50. Korneliussen TS, Albrechtsen A, Nielsen R (2014) ANGSD: Analysis of next generation sequencing data. BMC Bioinformatics 15, 356
51. Prada C et al (2014) Genetic species delineation among branching Caribbean Porites corals. Coral Reefs 33:1019–1030
52. Prada C et al (2016) Empty niches after extinctions increase population sizes of modern corals. Curr Biol 26:3190–3194
53. Babcock RC (1991) Comparative demography of three species of scleractinian corals using age- and size-dependent classifications. Ecol Monogr 61:225–244
54. Wickham H (2011) Ggplot2: Ggplot2. Wiley Interdiscip Rev Comput Stat 3:180–185
55. R Core Team (2022) R: A Language and Environment for Statistical Computing. R Foundation for Statistical Computing, Vienna, Austria
56. Hume BCC et al (2019) SymPortal: A novel analytical framework and platform for coral algal symbiont next-generation sequencing ITS2 profiling. Mol Ecol Resour 19:1063–1080
57. Dixon P (2003) VEGAN, a package of R functions for community ecology. J Veg Sci 14:927–930
58. Knaus BJ, Grünwald NJ (2017) vcfr: a package to manipulate and visualize variant call format data in R. Mol Ecol Resour 17:44–53
59. Browning BL, Tian X, Zhou Y, Browning SR (2021) Fast two-stage phasing of large-scale sequence data. Am J Hum Genet 108:1880–1890
60. Browning BL, Zhou Y, Browning SR (2018) A one-penny imputed genome from next-generation reference panels. Am J Hum Genet 103:338–348
61. Sabeti PC et al (2007) Genome-wide detection and characterization of positive selection in human populations. Nature 449:913–918
62. Voight BF, Kudaravalli S, Wen X, Pritchard J (2006) K. A map of recent positive selection in the human genome. PLoS Biol 4:e72
63. Ferrer-Admetlla A, Liang M, Korneliussen T, Nielsen R (2014) On detecting incomplete soft or hard selective sweeps using haplotype structure. Mol Biol Evol 31:1275–1291
64. Torres R, Szpiech ZA, Hernandez RD (2018) Human demographic history has amplified the effects of background selection across the genome. PLoS Genet 14:e1007387
65. Szpiech ZA, Hernandez RD, Selscan (2014) An efficient multithreaded program to perform EHH-based scans for positive selection. Mol Biol Evol 31:2824–2827
66. Szpiech Z (2025) A. Selscan v2.1
67. Cingolani P et al (2012) A program for annotating and predicting the effects of single nucleotide polymorphisms, SnpEff: SNPs in the genome of Drosophila melanogaster strain w1118; iso-2; iso-3. Fly (Austin) 6:80–92

68. Cingolani P et al (2012) Using Drosophila melanogaster as a model for genotoxic chemical mutational studies with a new program, SnpSift. Front Genet 3:35
69. Zhang C, Dong S-S, Xu J-Y, He W-M, Yang T-L (2019) PopLDdecay: a fast and effective tool for linkage disequilibrium decay analysis based on variant call format files. Bioinformatics 35:1786–1788
70. Korunes KL, Samuk K, pixy (2021) Unbiased estimation of nucleotide diversity and divergence in the presence of missing data. Mol Ecol Resour 21:1359–1368
71. Lambeck K (1996) Shoreline reconstructions for the Persian Gulf since the last glacial maximum. Earth Planet Sci Lett 142:43–57
72. Hume BCC et al (2015) Symbiodinium thermophilum sp. nov., a thermotolerant symbiotic alga prevalent in corals of the world's hottest sea, the Persian/Arabian Gulf. Sci Rep 5:8562
73. LaJeunesse TC et al (2014) Ecologically differentiated stress-tolerant endosymbionts in the dinoflagellate genusSymbiodinium(Dinophyceae) Clade D are different species. Phycologia 53:305–319
74. Fidler AL et al (2017) Collagen IV and basement membrane at the evolutionary dawn of metazoan tissues. Elife 6
75. McCall AS et al (2014) Bromine is an essential trace element for assembly of collagen IV scaffolds in tissue development and architecture. Cell 157:1380–1392
76. Ricaurte M, Schizas NV, Ciborowski P, Boukli NM (2016) Proteomic analysis of bleached and unbleached Acropora palmata, a threatened coral species of the Caribbean. Mar Pollut Bull 107:224–232
77. Barshis DJ et al (2013) Genomic basis for coral resilience to climate change. Proceedings of the National Academy of Sciences 110, 1387–1392
78. Kingsley D (1994) The TGF-b superfamily: new members, new receptors, and new genetic tests of function in different organisms. Genes Dev 8:133–146
79. Halloran D, Durbano HW, Nohe A (2020) Bone Morphogenetic Protein-2 in development and bone homeostasis. J Dev Biol 8
80. Fuess LE, Butler CC, Brandt ME, Mydlarz LD (2020) Investigating the roles of transforming growth factor-beta in immune response of Orbicella faveolata, a scleractinian coral. Dev Comp Immunol 107:103639
81. Detournay O, Schnitzler CE, Poole A, Weis VM (2012) Regulation of cnidarian-dinoflagellate mutualisms: Evidence that activation of a host TGFβ innate immune pathway promotes tolerance of the symbiont. Dev Comp Immunol 38:525–537
82. Bell SP (2002) The origin recognition complex: from simple origins to complex functions. Genes Dev 16:659–672
83. Nigg EA (1995) Cyclin-dependent protein kinases: key regulators of the eukaryotic cell cycle. BioEssays 17:471–480

84. Wood-Charlson EM, Hollingsworth LL, Krupp DA, Weis VM (2006) Lectin/glycan interactions play a role in recognition in a coral/dinoflagellate symbiosis. Cell Microbiol 8:1985–1993
85. Pinzón JH et al (2015) Whole transcriptome analysis reveals changes in expression of immune-related genes during and after bleaching in a reef-building coral. R Soc Open Sci 2:140214
86. Zhu Y, Li Q (2024) Multifaceted roles of PDCD6 both within and outside the cell. J Cell Physiol 239:e31235
87. Wang X et al (2016) KDELC1, a novel endoplasmic reticulum resident glycoprotein in hepatic dysfunction. Int J Clin Exp Med 9:10529–10536
88. Aguilar C et al (2019) Transcriptomic analysis reveals protein homeostasis breakdown in the coral Acropora millepora during hypo-saline stress. BMC Genomics 20:148
89. Klimovich A et al (2020) Prototypical pacemaker neurons interact with the resident microbiota. Proc. Natl. Acad. Sci. U. S. A. 117, 17854–17863
90. Nadir E, Benayahu Y, Ofek-Lalzar M, Gabrieli T, Lotan T (2025) Diffuse pacemaker mechanism with distinctive organization drives pulsation in the octocoral Xenia umbellata. Proc. Natl. Acad. Sci. U. S. A. 122, e2500611122
91. Michaely P, Bennett V (1992) The ANK repeat: a ubiquitous motif involved in macromolecular recognition. Trends Cell Biol 2:127–129
92. Takeshima H, Komazaki S, Nishi M, Iino M, Kangawa K (2000) Junctophilins Mol Cell 6:11–22
93. Pajares M (2017) Á. PDRG1 at the interface between intermediary metabolism and oncogenesis. World J Biol Chem 8:175–186
94. Lee I-G et al (2018) A conserved interaction of the dynein light intermediate chain with dynein-dynactin effectors necessary for processivity. Nat Commun 9:986
95. Mayorga LS, Cebrian I (2019) Rab22a: A novel regulator of immune functions. Mol Immunol 113:87–92
96. Zhang X et al (2021) DCAF11 supports targeted protein degradation by electrophilic proteolysis-targeting chimeras. J Am Chem Soc 143:5141–5149
97. Zhao X et al (2023) Alterations of the m6A methylation induced by TGF-β2 in ARPE-19 cells. Front Biosci (Landmark Ed) 28:148
98. Stankiewicz KH et al (2025) Heat-responsive dynamic shifts in alternative splicing of the coral Acropora cervicornis. bioRxiv 10.1101/2025.01.21.634199
99. Ciechanover A (2005) Proteolysis: from the lysosome to ubiquitin and the proteasome. Nat Rev Mol Cell Biol 6:79–87
100. Maor-Landaw K et al (2014) Gene expression profiles during short-term heat stress in the red sea coral Stylophora pistillata. Glob Chang Biol 20:3026–3035
101. Kaniewska P et al (2015) Transcriptomic changes in coral holobionts provide insights into physiological challenges of future climate and ocean change. PLoS ONE 10:e0139223

102. Burt JA (2024) From Phoenix to Sisyphus: Climate change impacts and intervention strategies for Arabian gulf coral reefs. J Coast Res 113
103. Howells EJ et al (2020) Corals in the hottest reefs in the world exhibit symbiont fidelity not flexibility. Mol Ecol 29:899–911
104. Riegl B, Purkis S (2015) Coral population dynamics across consecutive mass mortality events. Glob Chang Biol 21:3995–4005
105. Smith EG, Hume BCC, Delaney P, Wiedenmann J, Burt JA (2017) Genetic structure of coral-Symbiodinium symbioses on the world's warmest reefs. PLoS ONE 12:e0180169
106. Reynolds MR (1993) Physical oceanography of the Gulf, Strait of Hormuz, and the Gulf of Oman—Results from the Mt Mitchell expedition. Mar Pollut Bull 27:35–59
107. Terraneo TI et al (2019) Environmental latitudinal gradients and host-specificity shape Symbiodiniaceae distribution in Red Sea Porites corals. J Biogeogr 46:2323–2335
108. Matias AMA et al (2023) Cryptic diversity and spatial genetic variation in the coral Acropora tenuis and its endosymbionts across the Great Barrier Reef. Evol Appl 16:293–310
109. Marzonie MR, Nitschke MR, Bay LK, Bourne DG, Harrison HB (2024) Symbiodiniaceae diversity varies by host and environment across thermally distinct reefs. Mol Ecol 33:e17342
110. Strader ME, Aglyamova GV, Matz MV (2016) Red fluorescence in coral larvae is associated with a diapause-like state. Mol Ecol 25:559–569
111. Kenkel CD, Matz MV (2016) Gene expression plasticity as a mechanism of coral adaptation to a variable environment. Nat Ecol Evol 1:14
112. Riegl BM et al (2012) Coral bleaching and mortality thresholds in the SE gulf: Highest in the world. Coral Reefs of the World 95–105. Springer Netherlands, Dordrecht. doi:10.1007/978-94-007-3008-3_6.
113. Howells EJ et al (2016) Species-specific trends in the reproductive output of corals across environmental gradients and bleaching histories. Mar Pollut Bull 105:532–539
114. Burt JA et al (2020) Chapter 4. Status and Trends of Coral Reefs of the ROPME Sea Area
115. Knowlton N et al (2021) Rebuilding Coral Reefs: A Decadal Grand Challenge. http://dx.doi.org/10.53642/nrky9386 doi:10.53642/nrky9386
116. Peixoto RS, Alker A, Voolstra CR (2025) Bioengineering the coral holobiont: Evidence, hurdles, and pathways for rebuilding reefs. One Earth 8:101551
117. Gegner HM et al (2019) High levels of floridoside at high salinity link osmoadaptation with bleaching susceptibility in the cnidarian-algal endosymbiosis. Biol Open 8:bio045591
118. Gegner HM et al (2017) High salinity conveys thermotolerance in the coral model Aiptasia. Biol Open 6:1943–1948
119. Fiesinger A, Voolstra CR (2025) Signatures of host genomic and algal symbiont selection in the coral Porites harrisoni from the Persian/Arabian Gulf. https://doi.org/10.5281/ZENODO.17827487. Zenodo

120. Fiesinger A, Voolstra CR (2026) afiesinger/UAE_PAG_WGS_PopGen_Phar: UAE_PAG_WGS_PopGen_Phar (Zenodo, 2026). 10.5281/ZENODO.20732674

Figures

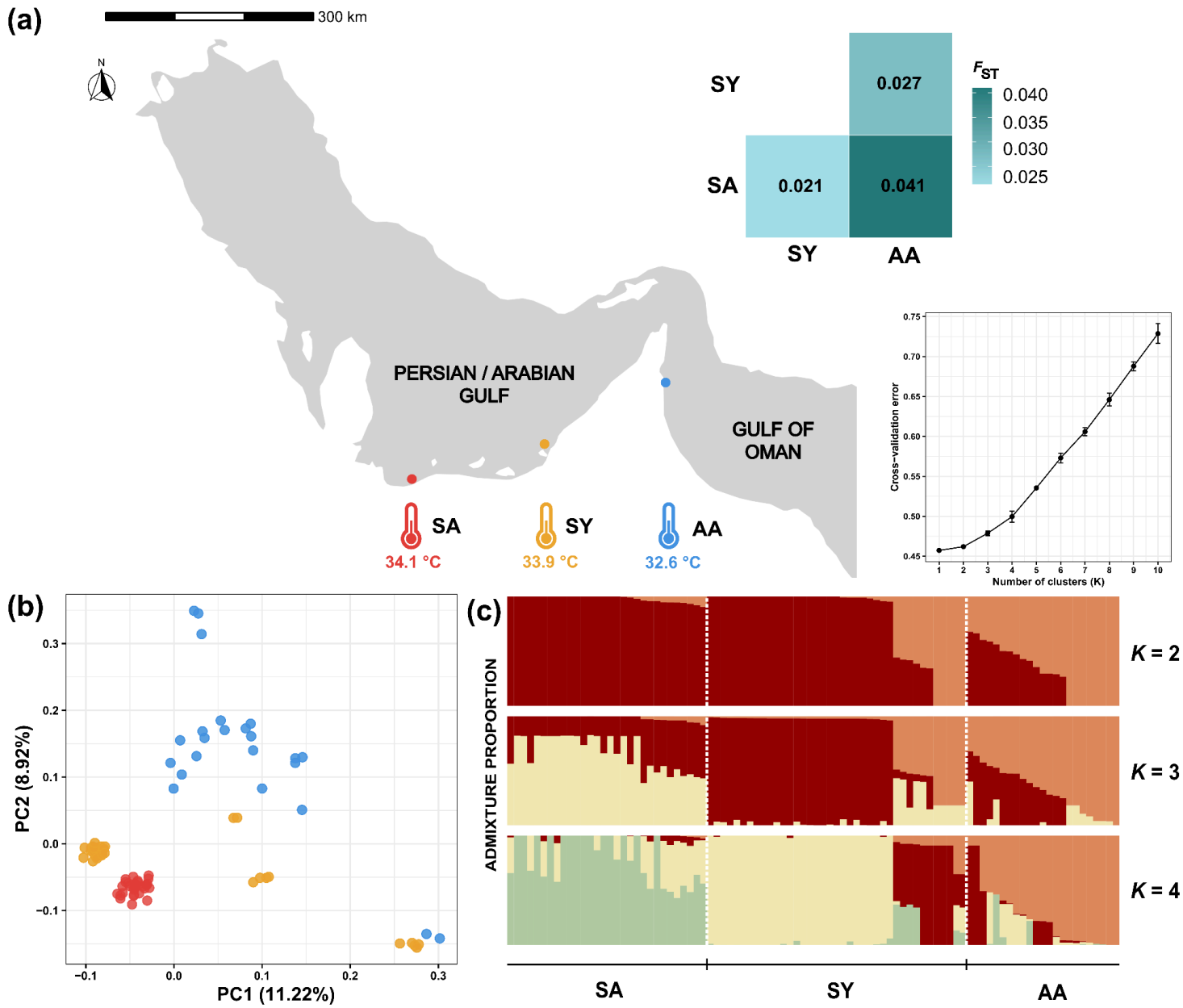


Figure 1

Population structure of *Porites harrisoni* in the PAG and GO. (a) Map with sampling locations, colors correspond to differing MMMs (34.1 °C at SA, 33.9 °C at SY, 32.6 °C at AA); inset: pairwise Weir & Cockerham's F_{ST} between sampling locations. **(b)** Principal component analysis (PCA) of the three sampling locations based on 663,850 SNPs. **(c)** ADMIXTURE results for *K* = 2 to 4 with the cross-

validation error plotted per cluster for all runs (*K* = 1 to 10; inset). Bars represent each individual colony, colored by cluster assignment. Site codes are: *SA* Saada Reef, *SY* Saadiyat Reef, *AA* Al Aqah.

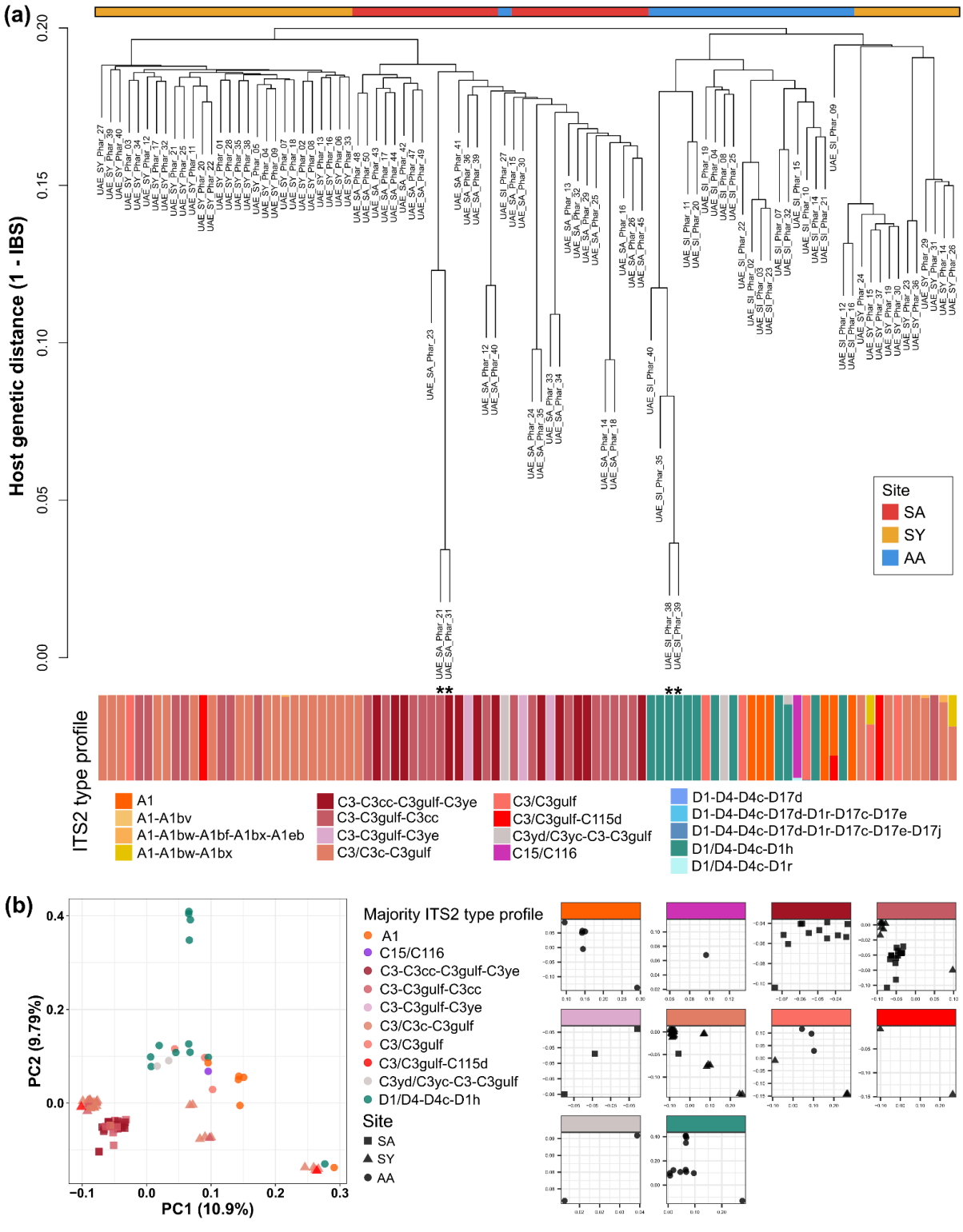


Figure 2

Relationship between host genetic distance and algal symbiont assemblage. (a) Hierarchical cluster dendrogram of host genotypes based on pairwise identity-by-state (IBS) values. Horizontal bars denote

host colony sampling location. The associated ITS2 type profiles for each coral colony as output by SymPortal are shown as barplots underneath. Asterisks denote clones identified by kinship analysis. **(b)**Principal component analysis (PCA) of coral host genetic variation color coded (left) and faceted (right) by majority ITS2 type profile of each colony of *P. harrisoni.* Shapes correspond to sampling location.

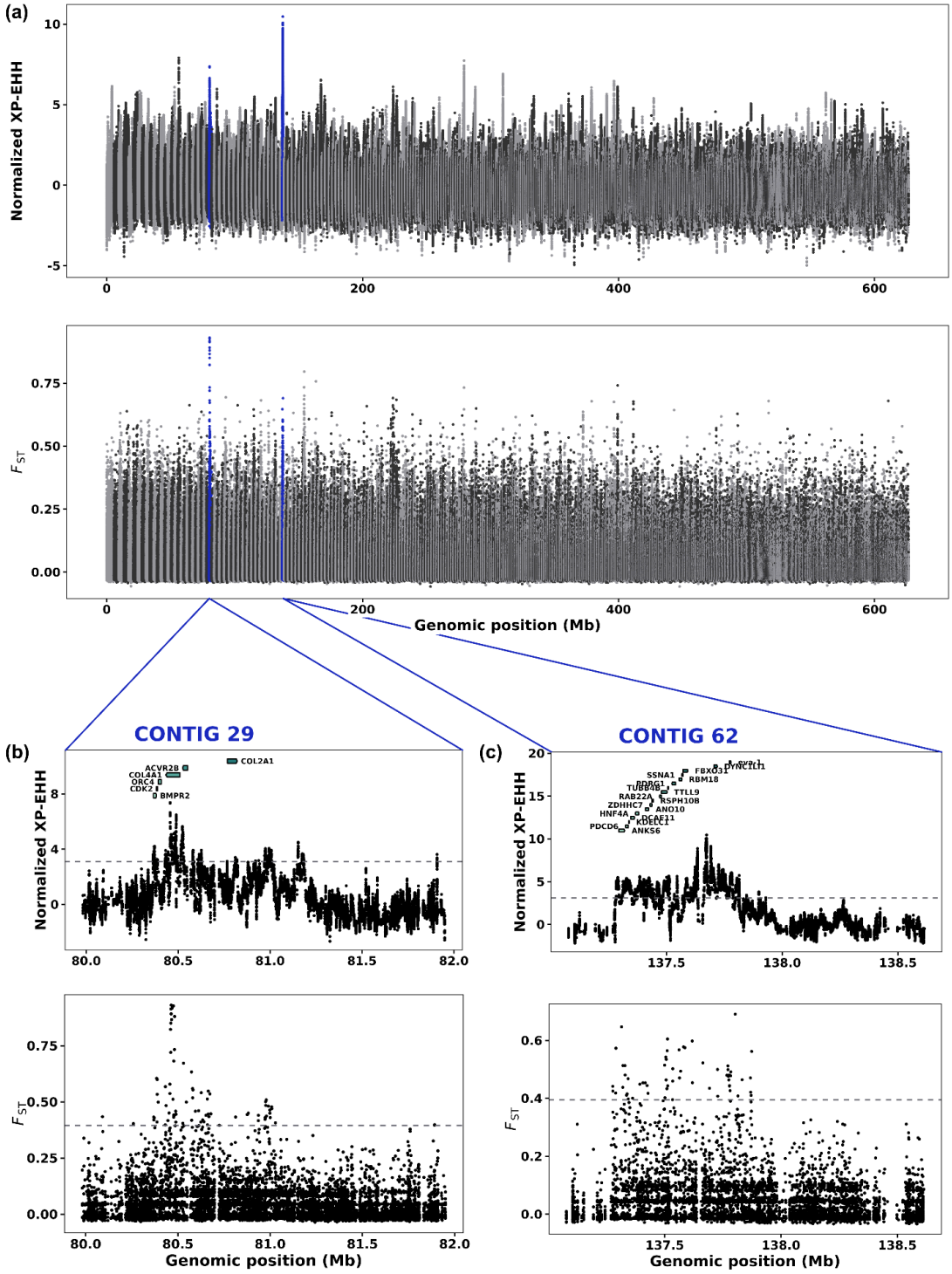


Figure 3

Candidate regions under positive selection in southern PAG *Porites harrisoni*. Manhattan plots of **(a)** normalized XP-EHH scores (top) and F_{ST} values (bottom) along the whole genome (626 Mb), with contigs displayed in alternating light and dark grey colors. In blue are the two candidate regions of selection, **(b)** contig 29 and **(c)** contig 62, with the respective annotated genes in the candidate regions under positive selection (green arrows) and top 1% (for XP-EHH) and top 0.1% (for F_{ST}) outlier thresholds (grey dashed lines) (Supplementary Tables S1 and S2).

Supplementary Files

This is a list of supplementary files associated with this preprint. Click to download.

- SuppMatTables.xlsx
- SuppMatFigs.docx